Synthesis, structure and properties of the macrocyclic ferrocenophanes with cyclopentadienyl ligands tethered by oligo(ethylene glycol) chain

Yuji Suzaki, Atsuko Takagi, Kohtaro Osakada*

Chemical Resources Laboratory (Mail Box R1-3), Tokyo Institute of Technology, 4259 Nagatsuta, Midori-ku, Yokohama 226-8503, Japan

ARTICLE INFO

ABSTRACT

Cyclization reactions of $Fe\{C_5H_4OCH_2(CH_2OCH_2)_nCH_2OTs\}_2$ (n = 1, 2) with C_6H_4-1,2-$(OH)_2$, C_6H_4-1,3-$(OH)_2$, and $Fe(C_5H_4OAc)_2$ under basic conditions yield the corresponding macrocyclic 1,1′-ferrocenophanes. The ferrocenophane having a pyrido-crown ether structure was also synthesized. These ferrocenophanes were characterized by X-ray crystallography and NMR spectroscopy. Cyclic voltammograms of the ferrocenophanes exhibited reversible redox peaks assigned to the oxidation and reduction of the ferrocene unit. The macrocyclic pyrido-containing ferrocenophane forms pseudorotaxane with $[NH_2\{(CH_2)_9Me\}_2]BARF$ (BARF = $B\{C_6H_3$-3,5-$(CF_3)_2\}_4$) in $CDCl_3$.

© 2010 Elsevier B.V. All rights reserved.

1. Introduction

Ferrocenophanes, ferrocene derivatives whose cyclopentadienyl ligands were connected by bridging unit, have received attention due to their unique propertied such as the intramolecular electronic communication, the ligandation to the transition metals and their ring-opening polymerization [1–5]. Macrocyclic ferrocenophanes having oligo(ethylene glycol) units as the tether of the cyclopentadienyl ligands were regarded as analogues to the crown ethers and have been reported to include metal cations as the host molecule [6]. The affinity to the metal cations varies depending on the length of the oligo(ethylene glycol) tether, oxidation state of the Fe atom, and the presence of a heteroatom within the ring [6–8].
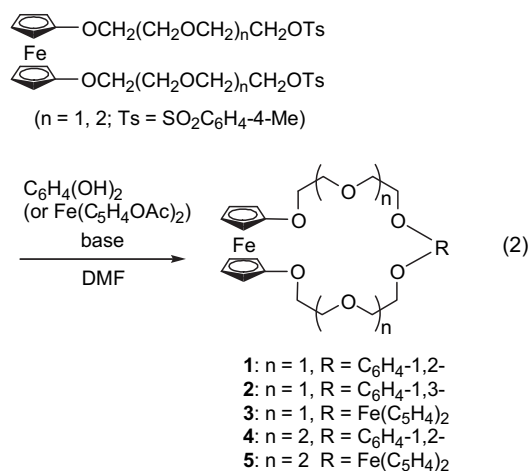
Recently we have reported a macrocyclic octaoxa[22]ferrocenophane and its rotaxane with dialkyl ammonium [9]. The rotaxane undergoes disaggregation reaction in CD_3CN (k_{obs} = 3.9 (7) $\times 10^{-6}$ s^{-1} at 45 °C) (Eq (1)), although the rotaxane having DB24C8 (dibenzo[24]crown-8) as a macrocyclic component is stable in solution under the same conditions. It is probably assigned to the larger size of the cavity of the octaoxa[22]ferrocenophane than that of DB24C8. The macrocyclic structures of these 1,1′-ferrocenylene-containing crown ethers were considered
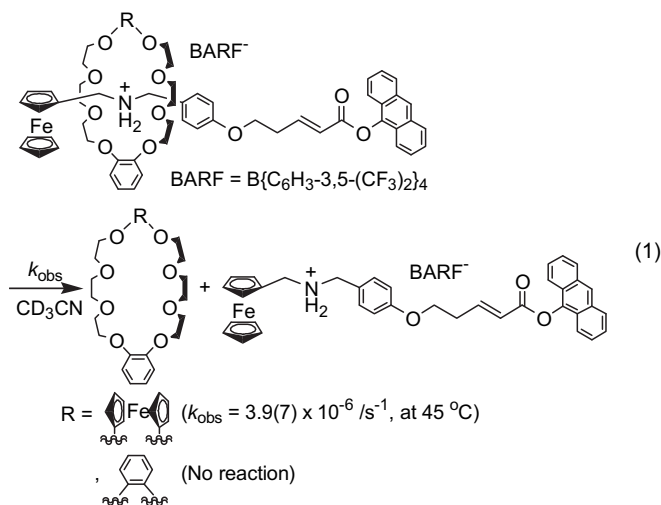
to influence the formation of the host–guest complexes with the cationic ions or molecules. Akabori reported detailed structure of the complex of a pentaoxa[13]ferrocenophane and NaSCN [6e]. In this paper we report preparation of macrocyclic 1,1′-ferrocenophanes as well as their structures in the solid state, electrochemical properties, and pseudorotaxane formation in solution.

* Corresponding author. Tel./fax: +81 45 924 5224.
  E-mail address: kosakada@res.titech.ac.jp (K. Osakada).

(2)

1: n = 1, R = C$_6$H$_4$-1,2-
2: n = 1, R = C$_6$H$_4$-1,3-
3: n = 1, R = Fe(C$_5$H$_4$)$_2$
4: n = 2, R = C$_6$H$_4$-1,2-
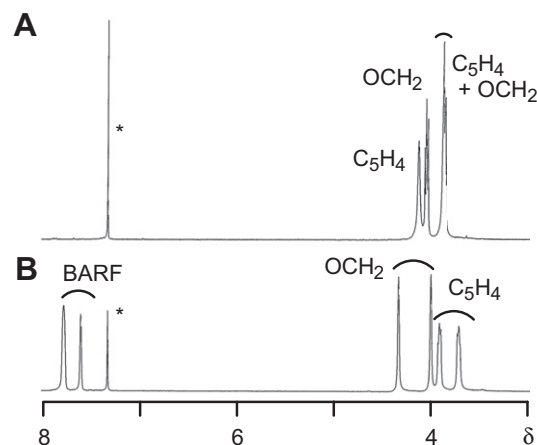**5**: n = 2 R = Fe(C$_5$H$_4$)$_2$

2. Results and discussion

Macrocyclic 1,1′-ferrocenophanes, **1**–**3** and **5**, were newly prepared, although **4** was already reported elsewhere [9]. Fe{C$_5$H$_4$OCH$_2$(CH$_2$OCH$_2$)$_n$CH$_2$OTs}$_2$ (n = 1, 2; Ts = SO$_2$C$_6$H$_4$-4-Me) is synthesized by reaction of TsCl and Fe{C$_5$H$_4$OCH$_2$(CH$_2$OCH$_2$)$_n$-CH$_2$OH}$_2$ (n = 1, 2) and used for the cyclization shown in Eq (2). Reaction of Fe(C$_5$H$_4$OCH$_2$CH$_2$OCH$_2$CH$_2$OTs)$_2$ and C$_6$H$_4$-1,2-(OH)$_2$ with K$_2$CO$_3$ in DMF for 7 days yields **1** having a hexaoxa[16]ferrocenophane structure (Table 1). FABMS (Fast atom bombardment mass spectrum) of **1** shows a peak at m/z = 468 corresponding to the structure. ^{13}C{^{1}H} NMR of **1** contains signals of C$_5$H$_4$ units (δ 56.1, 61.8, 126.7). Similar cyclization reactions yield ferrocene-containing crown ether **2**–**5** in 8–88% (Eq (2), Table 1). The reactions of Fe(C$_5$H$_4$OCH$_2$CH$_2$OCH$_2$CH$_2$OTs)$_2$ with C$_6$H$_4$-1,2-(OH)$_2$ and C$_6$H$_4$-1,3-(OH)$_2$ in the presence of K$_2$CO$_3$ yield **1** and **2** in higher yield (**1**:58%, **2**:20%) than those with Cs$_2$CO$_3$ (**1**:43%, **2**:13%). The difference in the yields was attributed to the template effect of the macrocycle to inclusion of metal cations, K$^+$ or Cs$^+$, which facilitates the cyclization.[10] Ferrocenophanes **3** and **5** were synthesized from the reaction of Fe{C$_5$H$_4$OCH$_2$(CH$_2$OCH$_2$)$_n$CH$_2$OTs}$_2$ (n = 1, 2) with [Fe(C$_5$H$_4$O)$_2$]$^{2-}$, generated in situ from Fe(C$_5$H$_4$OAc)$_2$, Cs$_2$CO$_3$ and KOH in water. ^{13}C{^{1}H} NMR spectrum of **3** contains three signals for C$_5$H$_4$ (δ 56.2, 62.1, 127.0) and two signals for OCH$_2$ (δ 70.1 (overlapping)) due to the symmetric structure composed of two 1,1′-ferrocenylenes and two di(ethylene glycol) units. ^{1}H NMR spectrum of **3** in CDCl$_3$ shows the two signals of the C$_5$H$_4$ hydrogens (δ 3.86–3.89, 4.11) as well as the two signals of OCH$_2$ (δ 3.86–3.89, 4.06) as shown in Fig. 1(A). Addition of NaBARF (BARF = B{C$_6$H$_3$-3,5-(CF$_3$)$_2$}$_4$) to a CDCl$_3$ solution of **3** ([**3**] = [NaBARF] = 10 mM) causes shift of the signals of OCH$_2$ (δ 3.86–3.89, 4.06) to lower

Fig. 1. ^{1}H NMR spectra (300 MHz, CDCl$_3$, r.t.) of (A) **3** ([**3**] = 10 mM) and (B) **3** and NaBARF ([**3**] = [NaBARF] = 10 mM). Peaks with asterisk indicate CHCl$_3$.

magnetic field position (δ 4.01, 4.33) and of C$_5$H$_4$ (δ 3.86–3.89, 4.11) to the higher magnetic field positions (δ 3.71, 3.92). FABMS of the mixture shows a peak at m/z = 599 corresponding to [**3** + Na]$^+$. These results indicate that **3** and Na$^+$ form the 1:1 inclusion complex in CDCl$_3$ solution [6,10].

Reaction of Fe(C$_5$H$_4$OCH$_2$CH$_2$OCH$_2$CH$_2$OH)$_2$ with C$_5$H$_3$N-2,6-(CH$_2$OTs)$_2$ in the presence of NaH ([Fe(C$_5$H$_4$OCH$_2$CH$_2$OCH$_2$CH$_2$OH)$_2$] = [C$_5$H$_3$N-2,6-(CH$_2$OTs)$_2$] = 5 mM) forms the cyclization product **6** in 18% isolated yield (Eq (3)). ^{13}C{^{1}H} NMR spectrum of **6** shows signals for the cyclopentadienyl carbons at δ 56.0, 62.9 and 128.8. FABMS of **6** shows a peak at m/z = 497 corresponding to the calculated molecular weight.

(3)
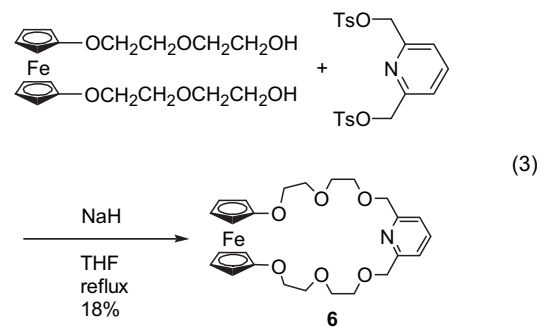
Recrystallization of **1**, **2** and **3** gave the single crystals suitable for X-ray structure analysis. Complexes of **5** with KBPh$_4$ and of **6** with NaBARF were also characterized by X-ray crystallography. The obtained molecular structures were shown in Fig. 2. C(C$_5$H$_4$)–O bonds of **1** (C5–O1 and C20–O6) adopt almost eclipsed conformation to the axis of the ferrocene unit (Chart 1(A), Table 2). The dihedral angle of the bonds, C5–O1 and C20–O6, is 16°. The conformations of C5–O1–C6 and C20–O6–C19 units avoid the electrostatic repulsion of the lone pairs of O1 and O6. Cyclopentadienyl ligands of **1** are deviated by 6.1(1)° from the ideal parallel conformation (Chart 1(B)) which is partly ascribed to the repulsion of O1 and O6. H8 atom of **1** has a contact with O3 (2.536 Å) which is shorter than the sum of the van der Waals radii for oxygen and hydrogen (2.72 Å), indicating the intramolecular hydrogen bond. Dihedral angles of C$_5$H$_4$ and C$_6$H$_4$ are almost vertical (86.33(9)° and 88.06(9)°). Distance between Fe1 and the centroid of C$_6$H$_4$ is 10.053 (1) Å. The circumferential bond lengths, the sum of the bond lengths of the macrocycle unit containing Fe1–C5–O1– through

Table 1
Conditions and yields of macrocyclic ferrocenophanes, **1**–**6**.

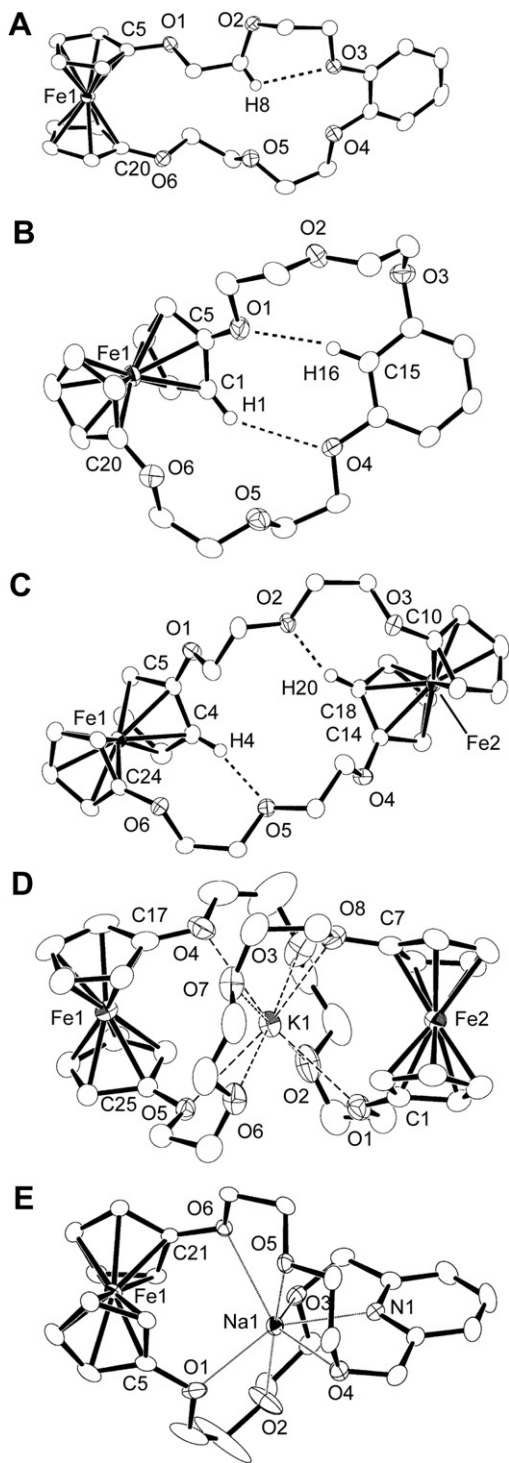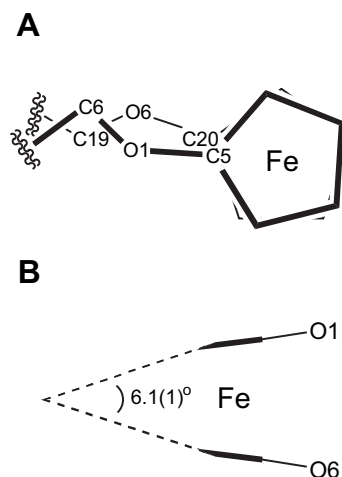| Compound	n	R	Base	Time	Isolated Yields
1	1	C$_6$H$_4$-1,2-	K$_2$CO$_3$	7 days	58%
			Cs$_2$CO$_3$	4 days	43%
2	1	C$_6$H$_4$-1,3-	K$_2$CO$_3$	3 days	20%
			Cs$_2$CO$_3$	3 days	13%
3	1	Fe(C$_5$H$_4$)$_2$	Cs$_2$CO$_3$/KOH	7 h	8%
4[a]	2	C$_6$H$_4$-1,2-	Cs$_2$CO$_3$	3 days	88%
5	2	Fe(C$_5$H$_4$)$_2$	Cs$_2$CO$_3$/KOH	19 h	33%
6[b]	–	–	NaH	2 days	18%

[a] Ref. [9].
[b] See Eq. (3) and experimental section for the structure of the compounds and reaction conditions.

Fig. 2. Molecular structure of (A) **1**, (B) **2**, (C) **3**, (D) [K(**5**)]BPh₄, and (E) [Na(**6**)]BARF. ORTEP drawings are shown in 50% probability except [Na(**6**)]BARF (30%). Hydrogen atoms and counter anions were omitted for simplicity.

Chart 1. Conformation of cyclopentadienyl ligands of **1** obtained from X-ray crystal analysis.

the cationic part of [K(**5**)]BPh₄. K1 atom was incorporated in the cavity of the two tri(ethylene glycol) units with helixed conformation. The distances between K1 and oxygen atoms of **5** (O1−O8) is in the range of 2.819(2)−2.888(2) Å. The atoms K1, Fe1 and Fe2 are arranged almost linearly, and K1 is located at the midpoint of Fe1 and Fe2 (distances: Fe1···K1, 4.122(1) Å, Fe2···K1, 4.114(1) Å; angle: Fe1···K1···Fe2, 174°). The dihedral angle of the cyclopentadienyl ligands between two ferrocenylene units is 57° (average). Fig. 2(E) shows the molecular structure of cationic part of [Na(**6**)]BARF. Na atom was incorporated in the cavity of **6**. The distance between Na1 and oxygens of **6** (O1−O6) is in the range of 2.419(2)−2.654(2) Å. The nitrogen atom of **6** coordinates to the Na atom (distance: Na1−N1, 3.914(1) Å; angle: Na1−N1···Centroid of C_5H_3N, 177°). Fe1 is separated from Na1 (distance: Fe1···Na1, 3.914 (1) Å), indicating little interaction between them. The dihedral angle of C5−O1 and C21−O6 bond is 50°.

In all the macrocyclic ferrocenophanes, cyclopentadienyl ligands of the ferrocenylene unit are in the eclipsed conformation (tilt angle: 0.9–14.5°) and the bond angles of $C(C_5H_4)$−O bonds were in the range of 16°−72°. The cyclopentadienyl ligands were almost parallel in **2**, **3**, **4**, [K(**5**)]BPh₄ and [Na(**6**)]BARF. The circumferential bond lengths were varied from 28.42(5) Å to 39.7 (1) Å depending on the ethylene glycol, the 1,1′-ferrocenylene, and the pyrido units[11,12]. Replacement of a C_6H_4-1,2- in the benzo-crown ether by a 1,1′-ferrocenylene unit causes the enlargement of the circumferential bond lengths by ca. 2.7 Å.

Ferrocene-containing crown ethers, **1**−**6**, undergo electrochemical oxidation and reduction at $E_{1/2}$ = −0.19 to −0.21 V (vs. Fc⁺/Fc, Fc = ferrocene). The redox potentials of the compounds determined by cyclic voltammetry (CV) are summarized in Table 3. The lower redox potentials of ferrocene-containing crown ethers were ascribed to the electron donation from the alkoxy groups to stabilize the Fe(III)⁺. Fig. 3 depicts cyclic voltammograms of **1** and **3** in MeCN. Both the compounds show one pair of peaks assigned to the redox of ferrocenylene units. The larger peaks of **3** than those of **1** indicate the oxidation and reduction of the two ferrocenylene units of **3** at the same potential and no interaction between the Fe centers. Similar redox peaks were observed also in the cyclic voltammogram of **5** ($E_{1/2}$ = −0.20 V).
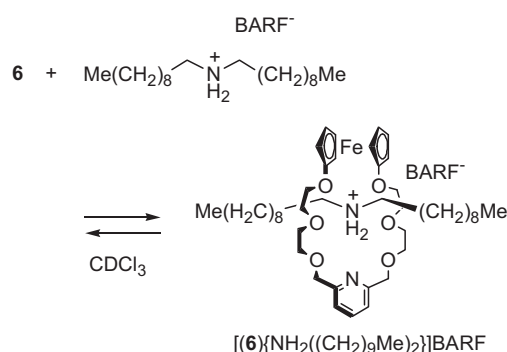
Formation of pseudorotaxane of **6** with di(alkyl)ammonium, [NH₂{(CH₂)₉Me}₂]BARF, was investigated by FABMS and ¹H NMR spectroscopy (Scheme 1). FABMS of the product obtained from the equimolar mixture of **6** and [NH₂{(CH₂)₉Me}₂]BARF in CDCl₃

−O6−C20−Fe1, is 28.42(5) Å which is longer than that of DB18C6 (dibenzo[18]crown-6, 25.8(2) Å) by 2.6 Å (Table 2)[11].

The compounds **2**, **3**, [K(**5**)]BPh₄ and [Na(**6**)]BARF were analyzed similarly. Intramolecular hydrogen bonds were observed in **2**, C1−H1···O4 (distance: 2.694 Å; angle: 144°) and C15−H16···O1 (distance: 2.600 Å; angle: 156°), and in **3**, C4-H4···O5 (distance: 2.725 Å; angle: 154°) and C18-H20···O2 (distance: 2.684 Å; angle: 153°) (Fig. 2(B) and (C)). Fig. 2(D) shows the molecular structure of

Table 2
Selected distances, bond angles of macrocyclic ferrocenophanes and crown ethers.

Compound	Angle of $C(C_5H_4)-O$ bonds	Dihedral angle of C_5H_4 planes/°[a]	Circumferential bond length/Å	Conformation of C_5H_4 planes (Tilt angle[b])
1	16°	6.1(1)	28.42(5)	eclipsed (8.7°)
2	62°	−1.60(8)	29.72(4)	eclipsed (0.9°)
3	72°	−2.55(7)	31.1(4)	eclipsed (1.2°)
	72°	−3.63(7)		
4	50°	3.92(9)	37.02(8)	eclipsed (14.5°)
5	57°	1.1(2)	39.7(1)	eclipsed (8.4°, 9.3°)
	58°	2.1(1)		
6	50°	1.6(1)	32.47(8)	eclipsed (6.0°)
DB18C6[c]	—	—	25.8(2)	—
DB24C8[d]	—	—	34.16(6)	—

[a] The deviations from the ideal parallel conformation.
[b] The deviations from the ideal eclipsed conformation.
[c] Ref. [11].
[d] Ref. [12].

Table 3
Redox potential of macrocyclic ferrocenophanes.[a]

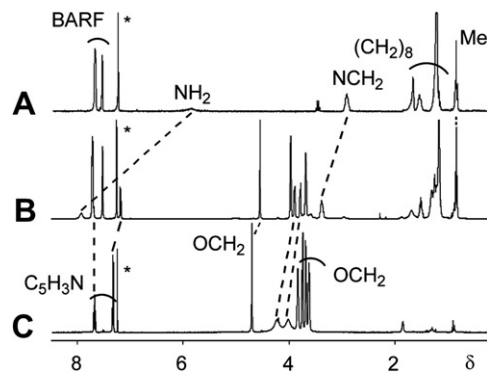| Compound	E_{pa}/V	E_{pc}/V	$E_{1/2}$ (ΔE[b])/V
1	−0.17	−0.24	−0.21 (0.07)
2	−0.18	−0.25	−0.21 (0.07)
3	−0.13	−0.25	−0.19 (0.12)
4[c]	−0.18	−0.24	−0.21 (0.06)
5	−0.16	−0.23	−0.20 (0.07)
6	−0.15	−0.28	−0.21 (0.13)

[a] Electrochemical potentials are obtained by cyclic voltammetry (CV) in MeCN containing $^nBu_4NPF_6$ as the electrolyte. Potentials are referenced with Fc^+/Fc (Fc = $Fe(C_5H_5)_2$). Sweep rate: 0.10 V s^{-1}.
[b] $\Delta E = E_{pa} - E_{pc}$.
[c] Ref. [9].

Scheme 1. Formation of pseudorotaxane of **6** and [NH$_2${(CH$_2$)9Me}$_2$]BARF.

contains a peak at $m/z = 796$ which is corresponding to the cationic pseudorotaxane, [(**6**){NH$_2$((CH$_2$)$_9$Me)$_2$}]$^+$. Addition of **6** to a CDCl$_3$ solution of [NH$_2${(CH$_2$)$_9$Me}$_2$]BARF ([**6**] = [[NH$_2${(CH$_2$)$_9$Me}$_2$] BARF] = 10 mM) causes shift of the ^{1}H NMR signals of NCH$_2$ (δ 2.94) and NH$_2$ (δ 5.88) hydrogens to the lower magnetic field positions (δ 3.38 (NCH$_2$), 7.92 (NH$_2$)) (Fig. 4(A) and (B)). Cooling the solution to −50 °C causes further shift of the NH$_2$ hydrogen peak to δ 8.42. The molar ratio of [(**6**){NH$_2$((CH$_2$)$_9$Me)$_2$}]BARF to [NH$_2${(CH$_2$)$_9$Me}$_2$] BARF at −50 °C was estimated to 87/13, based on the signal of the NCH$_2$ hydrogens. The shifts of the signals of [(**6**){NH$_2$((CH$_2$)$_9$Me)$_2$}] BARF from those of [NH$_2${(CH$_2$)$_9$Me}$_2$]BARF were ascribed to

the hydrogen bonds between NCH$_2$ and NH$_2$ hydrogen of [NH$_2${(CH$_2$)$_9$Me}$_2$]BARF and the oxygens and nitrogen of **6**[14].

The mixture of **6** and [NH$_2${(CH$_2$)$_9$Me}$_2$]BARF shows the signals of the hydrogen at C_6H_3N-CH_2 and 3-position of C_6H_3N of **6** (δ 4.55, 7.19) and the sharp cyclopentadienyl hydrogen signals (δ 3.80, 3.90) (Fig. 4(C)), while free **6** shows the former signals at lower positions (δ 4.72, 7.34) and as broad signals due to the cyclopentadienyl hydrogens (δ 4.03, 4.24). The difference in the ^{1}H NMR signals between the complexed and uncomplexed macrocycle is ascribed to the restricted ring motion in ferrocene unit in pseudorotaxane [(**6**){NH$_2$((CH$_2$)$_9$Me)$_2$}]BARF. The association constant K_a (5.1 × 10^3 M^{-1} at 25 °C) is obtained from the ^{1}H NMR and found to be larger than that of the complex of P21C7 (pyrido[21]crown-7) and

Fig. 3. Cyclic voltammograms in MeCN containing 0.10 M $^nBu_4NPF_6$ at 25 °C. Sweep rate: 0.10 V s^{-1}. (A) **1** (1.0 mM) and (B) **3** (1.0 mM).

Fig. 4. ^{1}H NMR spectra (300 MHz, CDCl$_3$, 25 °C) of (A) [NH$_2${(CH$_2$)$_9$Me}$_2$]BARF, (B) **6** and [NH$_2${(CH$_2$)$_9$Me}$_2$]BARF (10 mM for each), and (C) **6**. Peaks with asterisk indicate CHCl$_3$.

[NH$_2$(nBu)$_2$]PF$_6$ in acetone-d_6 (K_a = 1625 M^{-1} at 22 °C)[13]. Stoddart et al. investigated complexation of DB24C8 and di(n-alkyl) ammonium with PF$_6^-$ anion in CDCl$_3$ and concluded that low solubility of the dialkylammonium in the less polar solvent prevented determination of precise association constant[15]. Since di (alkyl)ammonium with BARF counter anion used in this study is soluble in CDCl$_3$ and forms an equilibrated mixture with the [2] pseudorotaxane, the ^{1}H NMR data gives the reliable association constants in CDCl$_3$. Similar pseudorotaxane formation of [NH$_2${(CH$_2$)$_9$Me}$_2$]BARF with 1–3 and 5 was not observed in both in ^{1}H NMR spectroscopy and in FABMS measurement.

In summary, we report the synthesis of macrocyclic ferrocenophanes which were analyzed by X-ray crystallography. The crown ethers with various ring sizes were obtained depending on the numbers of ethylene glycol units as well as the 1,1′-ferrocenylene, C$_6$H$_4$ and pyrido units. The obtained ferrocene-containing crown ethers exhibit reversible oxidation and reduction of the Fe(II) center at lower potentials than that of unsubstituted ferrocene. The macrocyclic ferrocenophanes having a pyrido group showed function as a host molecule for the dialkylammonium to form a pseudorotaxane type complex in solution.

3. Experimental

3.1. General

Fe{C$_5$H$_4$OCH$_2$(CH$_2$OCH$_2$)$_2$CH$_2$OTs}$_2$[9], Fe(C$_5$H$_4$OAc)$_2$[6c,16], C$_5$H$_3$N-2,6-(CH$_2$OTs)$_2$[17], NaBARF[18], (BARF = B{C$_6$H$_3$-3,5-(CF$_3$)$_2$}$_4$) and 4[9] were prepared according to the literature method. The other chemicals were commercially available. DMF and water used as solvent for preparation of Fe(C$_5$H$_4$OCH$_2$CH$_2$OCH$_2$CH$_2$OH)$_2$, 1, 2, 3 and 5 were degassed by N$_2$ gas bubbling (1 h) before use. NMR spectra (^{1}H, ^{13}C{^{1}H}) were recorded on a Varian MERCURY300. The chemical shifts were referenced with respect to CHCl$_3$ (δ 7.26) for ^{1}H and CDCl$_3$ (δ 77.0) for ^{13}C as internal standards. Fast atom bombardment mass spectrum (FABMS) was obtained from JEOL JMS-700 (matrix, 2-nitrophenyloctylether). Elemental analyses were carried out with a Yanaco MT-5 CHN autorecorder. Cyclic voltammetry (CV) was measured in MeCN solution containing 0.1 M ^{n}Bu$_4$NPF$_6$ with ALS Electrochemical Analyzer Model-600A. The measurement was carried out in a standard one-compartment cell equipped with Ag$^+$/Ag reference electrode, a platinum-wire counter electrode and a platinum-disk working electrode (ID: 1.6 mm). Thermogravity analysis (TGA) was recorded on Seiko TG/DTA6200R. Differential scanning calorimeter (DSC) was recorded on Seiko DSC6200S. IR absorption spectra were recorded on Shimadzu FT/IR-8100 spectrometers.

3.2. Fe(C$_5$H$_4$OCH$_2$CH$_2$OCH$_2$CH$_2$OH)$_2$

The aqueous solution (40 mL) containing Fe(C$_5$H$_4$OAc)$_2$ (0.73 g, 2.4 mmol), [18]crown-6 (0.021 g, 0.079 mmol) and KOH (6.9 g, 120 mmol) was refluxed for 20 min under nitrogen atmosphere. Cl (CH$_2$CH$_2$O)$_2$THP (THP = 2-tetrahydropyranyl) (2.0 g, 9.6 mmol) was added to the solution followed by further refluxing for 7 h. The product was extracted by Et$_2$O and the separated organic phase was washed with NaHCO$_3$(aq) and water then dried over MgSO$_4$, filtered and evaporated to give yellow oil. The crude product was purified by SiO$_2$ column chromatography (AcOEt, R_f = 0.08) to give Fe(C$_5$H$_4$OCH$_2$CH$_2$OCH$_2$CH$_2$OH)$_2$ as yellow oil (0.24 g, 0.61 mmol, 25%). Anal. Calcd. for C$_{18}$H$_{26}$FeO$_6$(H$_2$O)$_{0.75}$: C, 53.02; H, 6.80. Found: C, 53.14; H, 6.58; ^{1}H NMR (300 MHz, CDCl$_3$, r.t.): δ 2.99 (m, 2H, OH), 3.64–3.67 (m, 4H, CH$_2$), 3.73–3.79 (m, 8H, CH$_2$), 3.88 (brs, 4H, C$_5$H$_4$), 3.99–4.02 (brs, 4H, C$_5$H$_4$); ^{13}C{^{1}H} NMR (75.5 MHz, CDCl$_3$,

r.t.): δ 55.9 (C$_5$H$_4$), 61.4 (CH$_2$), 62.3 (C$_5$H$_4$), 69.6 (CH$_2$, 2 signals), 72.6 (CH$_2$), 126.5 (C$_5$H$_4$).

3.3. Fe(C$_5$H$_4$OCH$_2$CH$_2$OCH$_2$CH$_2$OTs)$_2$

NaOH (0.15 g, 3.3 mmol) and TsCl (0.26 g, 1.3 mmol) was added to a solution (THF/H$_2$O = 0.6 mL/0.1 mL) of Fe(C$_5$H$_4$OCH$_2$CH$_2$OCH$_2$CH$_2$OH)$_2$ (0.17 g, 0.43 mmol) at room temperature. The solution was stirred for 21 h at room temperature followed by addition of water and the extraction of the product with CH$_2$Cl$_2$. The separated organic phase was dried over MgSO$_4$, filtered, and evaporated to give Fe(C$_5$H$_4$OCH$_2$CH$_2$OCH$_2$CH$_2$OTs)$_2$ as orange oil (0.30 g, 0.42 mmol, 98%). Anal. Calcd. for C$_{32}$H$_{38}$FeO$_{10}$S$_2$(H$_2$O): C, 53.33; H, 5.59. Found: C, 53.25; H, 5.56; ^{1}H NMR (300 MHz, CDCl$_3$, r.t.): δ 2.42 (s, 6H, CH$_3$), 3.68–3.75 (m, 8H, CH$_2$), 3.83–3.85 (m, 4H, C$_5$H$_4$), 3.89–3.92 (m, 4H, CH$_2$), 4.07–4.08 (m, 4H, C$_5$H$_4$), 4.16–4.19 (m, 4H, CH$_2$), 7.32 (d, 4H, C$_6$H$_4$, J = 8 Hz), 7.79 (d, 4H, C$_6$H$_4$, J = 8 Hz); ^{13}C{^{1}H} NMR (75.5 MHz, CDCl$_3$, r.t.): δ 21.5 (CH$_3$), 55.8 (C$_5$H$_4$), 62.3 (C$_5$H$_4$), 68.6 (CH$_2$), 69.1 (CH$_2$), 69.5 (CH$_2$), 69.8 (CH$_2$), 126.4 (C$_5$H$_4$), 127.8 (C$_6$H$_4$), 129.7 (C$_6$H$_4$), 132.5 (C$_6$H$_4$), 144.7 (C$_6$H$_4$).

3.4. Ferrocenophane 1

A DMF solution (20 mL) containing Fe(C$_5$H$_4$OCH$_2$CH$_2$OCH$_2$CH$_2$OTs)$_2$ (0.23 g, 0.33 mmol) and ortho-catechol (36 mg, 0.33 mmol) was added dropwise to the DMF suspension (20 mL) of K$_2$CO$_3$ (0.46 g, 3.3 mmol) at 80 °C. The resulting solution was stirred for 7 days at 80 °C followed by evaporation. The obtained brown oil was dissolved in CH$_2$Cl$_2$ and the solution was washed with saturated NH$_4$Cl(aq). The separated organic phase was dried over MgSO$_4$, filtered and evaporated to form yellow oil. The crude product was purified by SiO$_2$ column chromatography (CH$_2$Cl$_2$, R_f = 0.09) to give 1 as yellow solid (90 mg, 0.19 mmol, 58%). Anal. Calcd. for C$_{24}$H$_{28}$FeO$_6$: C, 61.55; H, 6.03. Found: C, 61.43; H, 5.68; FABMS: Calcd. for C$_{24}$H$_{28}$FeO$_6$: 468. Found: m/z = 468; ^{1}H NMR (300 MHz, CDCl$_3$, r.t.): δ 3.81–3.83 (m, 4H, C$_5$H$_4$), 3.96–3.99 (m, 8H, CH$_2$), 4.03–4.06 (m, 4H, CH$_2$), 4.12–4.13 (m, 4H, C$_5$H$_4$), 4.19–4.22 (m, 4H, CH$_2$), 6.87–6.94 (m, 4H, C$_6$H$_4$); ^{13}C{^{1}H} NMR (75.5 MHz, CDCl$_3$, r.t.): δ 56.1 (C$_5$H$_4$), 61.8 (C$_5$H$_4$), 69.3 (CH$_2$), 69.8 (CH$_2$), 70.0 (CH$_2$), 70.6 (CH$_2$), 113.5 (C$_6$H$_4$), 121.3 (C$_6$H$_4$), 126.7 (C$_5$H$_4$), 148.6 (C$_6$H$_4$); IR (KBr disk, r.t., in cm^{-1}): 2938, 2679, 1356, 1279, 1125; 5% weight loss temperature: 262 °C (by TGA. scan rate = 5 °C/min); m.p.: 132 °C (by DSC. decomp.). Similar reaction using Cs$_2$CO$_3$ instead of K$_2$CO$_3$ gave 1 in 43% yield.

3.5. Ferrocenophane 2

A DMF solution (50 mL) containing Fe(C$_5$H$_4$OCH$_2$CH$_2$OCH$_2$CH$_2$OTs)$_2$ (0.27 g, 0.39 mmol) and meta-resorcinol (1,3-dihydroxybenzene) (46 mg, 0.39 mmol) was added dropwise to the DMF suspension (25 mL) of K$_2$CO$_3$ (0.54 g, 3.9 mmol) for 6 h at 80 °C. The resulting solution was stirred for 3 days at 80 °C followed by evaporation. The obtained brown oil was dissolved in CH$_2$Cl$_2$ and the solution was washed with saturated NH$_4$Cl(aq). The separated organic phase was dried over MgSO$_4$, filtered and evaporated to form yellow oil. The crude product was purified by SiO$_2$ column chromatography (CH$_2$Cl$_2$, R_f = 0.36) to give 2 as yellow solid (37 mg, 0.079 mmol, 20%). Anal. Calcd. for C$_{24}$H$_{28}$FeO$_6$: C, 61.55; H, 6.03 Found: C, 61.45; H, 5.90; FABMS: Calcd. for C$_{24}$H$_{28}$FeO$_6$: 468. Found: m/z = 468; ^{1}H NMR (300 MHz, CDCl$_3$, r.t.): δ 3.79 (t, 4H, CH$_2$, J = 4 Hz), 3.85 (m, 8H, CH$_2$, C$_5$H$_4$), 3.97 (t, 4H, CH$_2$, J = 4 Hz), 4.12 (brs, 4H, C$_5$H$_4$), 4.24 (t, 4H, CH$_2$, J = 5 Hz), 6.53 (dd, 2, C$_6$H$_4$, J = 8, 2 Hz), 6.89 (t, 1H, C$_6$H$_4$, J = 2 Hz), 7.14 (t, 1H, C$_6$H$_4$, J = 8 Hz); ^{13}C{^{1}H} NMR (75.5 MHz, CDCl$_3$, r.t.): δ 56.3 (C$_5$H$_4$), 62.3 (C$_5$H$_4$), 68.2 (CH$_2$), 69.9 (CH$_2$), 70.0 (CH$_2$), 70.2 (CH$_2$), 103.2 (C$_6$H$_4$), 108.3 (C$_6$H$_4$), 129.7

(C_6H_4), 160.0 (C_6H_4). Similar reaction using Cs_2CO_3 instead of K_2CO_3 gave **2** in 13% yield.

3.6. Ferrocenophane 3

The water suspension (8 mL) of Cs_2CO_3 (0.75 g, 2.3 mmol), KOH (0.10 g, 0.19 mmol), and $Fe(C_5H_4OAc)_2$ (70 mg, 0.23 mmol) was refluxed for 20 min under Ar atmosphere. A DMF solution (27 mL) containing $Fe(C_5H_4OCH_2CH_2OCH_2CH_2OTs)_2$ (0.16 g, 0.23 mmol) was added dropwise to the solution at 80 °C. The resulting solution was stirred for 7 h at 80 °C followed by evaporation. The obtained brown oil was dissolved in CH_2Cl_2 and the solution was washed with saturated NH_4Cl(aq). The separated organic phase was dried over $MgSO_4$, filtered and evaporated to form yellow oil. The crude product was purified by SiO_2 column chromatography (CH_2Cl_2, $R_f = 0.35$) to give **3** as yellow oil (10 mg, 0.017 mmol, 8%). Anal. Calcd. for $C_{28}H_{32}Fe_2O_6(H_2O)_{0.25}$: C, 57.91; H, 5.64. Found: C, 57.87; H, 5.30; FABMS: Calcd. for $C_{28}H_{32}Fe_2O_6$: 576. Found: $m/z = 576$; ^1H NMR (300 MHz, CDCl$_3$, r.t.): δ 3.86–3.89 (m, 16H, C_5H_4, CH_2), 4.06 (m, 8H, CH_2), 4.11 (m, 8H, C_5H_4); $^{13}C\{^1H\}$ NMR (75.5 MHz, CDCl$_3$, r.t.): δ 56.2 (C_5H_4), 62.1 (C_5H_4), 70.1 (CH_2, 2 signals), 127.0 (C_5H_4).

3.7. Ferrocenophane 5

The water suspension (10 mL) of Cs_2CO_3 (1.2 g, 3.6 mmol), KOH (0.19 g, 3.0 mmol) and $Fe(C_5H_4OAc)_2$ (0.12 g, 0.36 mmol) was refluxed for 20 min under Ar atmosphere. A DMF solution (60 mL) containing $Fe\{C_5H_4OCH_2(CH_2OCH_2)_2CH_2OTs\}_2$ (0.28 g, 0.36 mmol) was added dropwise to the solution at 80 °C. The resulting solution was stirred for 19 h at 80 °C followed by evaporation. The obtained brown oil was dissolved in CH_2Cl_2 and the solution was washed with saturated NH_4Cl(aq). The separated organic phase was dried over $MgSO_4$, filtered and evaporated to form **5** as yellow oil (80 mg, 0.12 mmol, 33%). The isolation of **5** was not feasible due to decomposition during the further purification by SiO_2 column chromatography and the preparative HPLC (eluent: CHCl$_3$). FABMS: Calcd. for $C_{32}H_{40}Fe_2O_8$: 664. Found: $m/z = 664$; ^1H NMR (300 MHz, CDCl$_3$, r.t.): δ 3.58–3.88 (m, 24H, CH_2), 3.83–3.88 (m, 8H, C_5H_4), 3.92–4.04 (m, 8H, CH_2), 4.09–4.18 (m, 8H, C_5H_4). Low stability of **5** in CDCl$_3$ prevents $^{13}C\{^1H\}$ NMR measurement.

3.8. Ferrocenophane 6

A THF solution (14 mL) containing $Fe(C_5H_4OCH_2CH_2OCH_2-CH_2OH)_2$ (107 mg, 0.27 mmol) and $C_5H_3N-2,6-(CH_2OTs)_2$ (120 mg, 0.27 mmol) was added dropwise for 24 h to the THF solution (43 mL) of NaH (19 mg, 0.81 mmol) under reflux. The solution was refluxed further 2 days followed by quenching with methanol/water and evaporation. The product was dissolved in AcOEt and the solution was washed with saturated NaCl(aq). The separated organic phase was dried over $MgSO_4$, filtered and evaporated to form yellow oil which was purified by SiO_2 column chromatography (AcOEt, $R_f = 0.19$) and preparative HPLC (eluent: CHCl$_3$) to give **6** as yellow solid (23 mg, 0.048 mmol, 18%). FABMS: Calcd. for $C_{25}H_{31}FeNO_6$: 497. Found: $m/z = 497$; ^1H NMR (400 MHz, CDCl$_3$, r.t.): 3.64 (brs, 4H, OCH$_2$), 3.70 (m, 4H, OCH$_2$), 3.77 (m, 4H, OCH$_2$), 3.85 (brs, 4H, OCH$_2$), 4.03 (brs, 4H, C_5H_4), 4.24 (brs, 4H, C_5H_4), 4.72 (s, 4H, $CH_2C_5H_3N$), 7.34 (d, 2H, C_3H_5N-H3, $J = 8$ Hz), 7.69 (t, 1H, C_3H_5N-H4, $J = 8$ Hz); $^{13}C\{^1H\}$ NMR (100 MHz, CDCl$_3$, r.t.): δ 56.0 (C_5H_4), 62.9 (C_5H_4), 69.8 (OCH$_2$), 69.8 (OCH$_2$), 70.0 (OCH$_2$), 71.0 (OCH$_2$), 74.3 ($CH_2C_5H_3N$), 121.2 (C_3H_5N-C3), 128.8 (C_5H_4), 137.1 (C_3H_5N-C4), 157.8 (C_3H_5N-C2); Anal. Calcd. for $C_{57}H_{43}BF_{24}FeNNaO_6$ ([Na(**6**)]BARF): C, 49.48; H, 3.13; N, 1.01. Found: C, 49.10; H, 2.77; N, 1.00; IR data for [Na(**6**)]BARF (KBr disk, r.t., in cm^{-1}): 2915, 1354, 1279, 1100–1170; 5% weight loss temperature: 327 °C (by TGA. scan rate = 5 °C/min).

3.9. [NH$_2${(CH$_2$)$_9$Me}$_2$]BARF

[NH$_2${(CH$_2$)$_9$Me}$_2$]BARF was prepared by similar method to the literature [19]. Data of [NH$_2${(CH$_2$)$_9$Me}$_2$]BARF: ^1H NMR (300 MHz, CDCl$_3$, r.t.): δ 0.87 (t, 6H, CH$_3$, $J = 7$ Hz), 1.16–1.36 (brs, 28H, CH$_2$), 1.51–1.62 (brs, 4H, NCH$_2$CH_2), 2.94 (m, 4H, NCH$_2$), 5.88 (brs, 2H, NH$_2$), 7.56 (s, 4H, p-C$_6$H$_3$(CF$_3$)$_2$), 7.70 (s, 8H, o-C$_6$H$_3$(CF$_3$)$_2$); $^{13}C\{^1H\}$ NMR (75.5 MHz, CDCl$_3$, r.t.): δ 13.9 (CH$_3$), 22.6 (CH$_2$), 25.9 (CH$_2$), 26.3 (CH$_2$), 28.6 (CH$_2$), 29.0 (CH$_2$), 29.1 (CH$_2$), 29.2 (CH$_2$), 31.7 (CH$_2$), 49.7 (NCH$_2$), 117.6 (p-C$_6$H$_3$), 124.6 (q, CF$_3$, J(FC) = 273 Hz), 128.9 (q, CCF$_3$, J(FC) = 32 Hz), 134.8 (o-C$_6$H$_3$), 161.7 (q, BC, J(BC) = 50 Hz); IR (neat, r.t., in cm^{-1}): 2934, 2860, 1356, 1279, 1129.

3.10. X-ray structure analyses

Crystals of **1**, **2** and **3** suitable for X-ray diffraction study were obtained by recrystallization from acetone, CH_2Cl_2/hexane, and

Table 4
Crystal data and details of structure refinement of **1**, **2**, **3**, [K(**5**)]BPh$_4$ and [Na(**6**)]BARF.

Compound	1	2	3	[K(**5**)]BPh$_4$	[Na(**6**)]BARF
recrystallization solvent	acetone	CH_2Cl_2/hexane	AcOEt	MeOH/acetone	AcOEt
color of crystal	orange	orange	orange	orange	orange
formula	$C_{24}H_{28}FeO_6$	$C_{24}H_{28}FeO_6$	$C_{28}H_{32}Fe_2O_6$	$C_{56}H_{60}Fe_2KO_8$	$C_{57}H_{43}NO_6BF_{24}FeNa$
molecular weight	468.33	468.33	576.25	1022.69	1383.58
crystal system	monoclinic	monoclinic	monoclinic	triclinic	triclinic
space group	$P2_1/n$ (No. 14)	$P2_1/n$ (No. 14)	$P2_1/n$ (No. 14)	$P\bar{1}$ (No. 2)	$P\bar{1}$ (No. 2)
a/Å	9.154(2)	13.994(2)	13.3096(7)	10.435(2)	12.527(3)
b/Å	13.057(3)	9.3331(15)	11.5137(6)	14.310(3)	12.978(3)
c/Å	17.934(4)	16.386(3)	16.1874(12)	16.747(4)	18.950(5)
α/deg	–	–	–	80.722(6)	98.513(4)
β/deg	102.716(4)	95.019(2)	92.094(4)	86.568(8)	105.126(3)
γ/deg	–	–	–	85.891(7)	94.139(3)
V/Å^3	2090.9(8)	2131.9(6)	2478.9(3)	2458.7(10)	2921(1)
Z	4	4	4	2	2
$F(000)$	984.00	984.00	1200.00	1072.00	1383.58
$D \cdot c$/g cm^{-1}	1.488	1.459	1.544	1.381	1.573
crystal size/mm	$0.70 \times 0.30 \times 0.15$	$0.20 \times 0.15 \times 0.10$	$0.40 \times 0.40 \times 0.20$	$0.80 \times 0.60 \times 0.15$	$0.50 \times 0.40 \times 0.20$
unique reflections	4659	4833	5389	10390	12307
used reflections [$I \geq 2.0\sigma$ (I)]	3448	3846	4850	8801	10566
No. of variables	308	308	357	673	863
R	0.032	0.029	0.027	0.052	0.050
R_w	0.036	0.036	0.040	0.064	0.080
good of fitness	1.01	1.02	0.96	1.04	0.90

AcOEt, respectively. The crystal of [K(**5**)]BPh$_4$ and [Na(**6**)]BARF was obtained by recrystallization from the solution containing **5** and KBPh$_4$ and from the solution containing **6** and NaBARF in 1:1 M ratio. All measurements were made on Rigaku AFC-10R Saturn CCD diffractometer with graphite monochromated Mo-Kα radiation. Calculations were carried out by using a program package Crystal Structure™ for Windows [20]. Crystal data and detailed results of refinement are summarized in Table 4. All hydrogen atoms were included at the calculated positions with fixed thermal parameters.

Acknowledgments

Appendix A. Supplementary material

CCDC nos. 787554, 787555, 787556, 787557, and 773746 contain the supplementary crystallographic data for **1**, **2**, **3**, [K(**5**)]BPh$_4$ and [Na(**6**)]BARF, respectively. These data can be obtained free of charge from The Cambridge Crystallographic Data Centre *via* www.ccdc.cam.ac.uk/data_request/cif.

References

[1] A. Togni, T. Hayashi (Eds.), Ferrocenes, VCH, New York, 1995.
[2] (a) P. Nguyen, P. Gómez-Elipe, I. Manners, Chem. Rev. 99 (1999) 1515;
(b) T.J. Colacot, Chem. Rev. 103 (2003) 3101.
[3] Recent example of the ferrocenophanes as the ligands for the transition metal complexes: (a) Y. Imamura, T. Mizuta, K. Miyoshi, Organometallics 25 (2006) 882;
(b) N. Fleury-Brégeot, A. Panossian, A. Chiaroni, A. Marinetti, Eur. J. Inorg. Chem. (2007) 3853;
(c) A. Almássy, K. Barta, G. Franciò, R. Šebesta, W. Leitner, Š Toma, Tetrahedron: Asymmetry 18 (2007) 1893.
[4] K. Osakada, T. Sakano, M. Horie, Y. Suzaki, Coord. Chem. Rev. 250 (2006) 1012.
[5] (a) I. Yamaguchi, T. Sakano, H. Ishii, K. Osakada, T. Yamamoto, J. Organomet. Chem. 584 (1999) 213;
(b) T. Sakano, H. Ishii, I. Yamaguchi, K. Osakada, T. Yamamoto, Inorg. Chim. Acta 296 (1999) 176;
(c) T. Sakano, M. Horie, K. Osakada, H. Nakao, Bull. Chem. Soc. Jpn. 74 (2001) 2059;
(d) M. Horie, T. Sakano, K. Osakada, H. Nakao, Organometallics 23 (2004) 18;
(e) T. Sakano, M. Horie, K. Osakada, H. Nakao, Eur. J. Inorg. Chem. (2005) 644;
(f) Y. Suzaki, M. Horie, T. Sakano, K. Osakada, J. Organomet. Chem. 691 (2006) 3403.
[6] (a) J.F. Biernat, T. Wilczewski, Tetrahedron 36 (1980) 2521;
(b) S. Akabori, H. Fukuda, Y. Habata, M. Sato, S. Ebine, Chem. Lett. (1982) 1393;
(c) S. Akabori, Y. Habata, Y. Sakamoto, M. Sato, S. Ebine, Bull. Chem. Soc. Jpn. 56 (1983) 537;
(d) S. Akabori, Y. Habata, M. Sato, S. Ebine, Bull. Chem. Soc. Jpn. 56 (1983) 1459;
(e) S. Akabori, Y. Habata, M. Sato, Bull. Chem. Soc. Jpn. 57 (1984) 68.
[7] (a) T. Saji, Chem. Lett. (1986) 275;
(b) T. Saji, I. Kinoshita, J. Chem. Soc., Chem. Commun. (1986) 716.
[8] 1,1'-Ferrocenylene-containing (pyrido)crown ethers having C$_5$H$_4$–COO bonds.
(a) T. Izumi, T. Tezuka, S. Yusa, A. Kasahara, Bull. Chem. Soc. Jpn. 57 (1984) 2435;
(b) T. Izumi, S. Murakami, A. Kasahara, Bull. Chem. Soc. Jpn. 61 (1988) 3565.
[9] Y. Suzaki, E. Chihara, A. Takagi, K. Osakada, Dalton Trans. (2009) 9881.
[10] C.J. Pedersen, J. Am. Chem. Soc. 89 (1967) 7017.
[11] G.M. de Lima, J.L. Wardell, W.T.A. Harrison, Acta Crystallogr. E64 (2008) o2001.
[12] I.R. Hanson, D.L. Hughes, M.R. Truter, J. Chem. Soc., Perkin Trans. 2 (1976) 972.
[13] C. Zhang, K. Zhu, S. Li, J. Zhang, F. Wang, M. Liu, N. Li, F. Huang, Tetrahedron Lett. 49 (2008) 6917.
[14] (a) G. Bottari, F. Dehez, D.A. Leigh, P.J. Nash, E.M. Pérez, J.K.Y. Wong, F. Zerbetto, Angew. Chem. Int. Ed. 42 (2003) 5886;
(b) T. Chang, A.M. Heiss, S.J. Cantrill, M.C.T. Fyfe, A.R. Pease, S.J. Rowan, J.F. Stoddart, A.J.P. White, D.J. Williams, Org. Lett. 2 (2000) 2947;
(c) A.R. Williams, B.H. Northrop, K.N. Houk, J.F. Stoddart, D.J. Williams, Chem. Eur. J. 10 (2004) 5406.
[15] P.R. Ashton, P.J. Campbell, E.J.T. Chrystal, P.T. Glink, S. Menzer, D. Philp, N. Spencer, J.F. Stoddart, P.A. Tasker, D.J. Williams, Angew. Chem., Int. Ed. Engl. 34 (1995) 1865.
[16] A.N. Nesmejanow, W.A. Ssasonowa, V.N. Drosd, Chem. Ber. 93 (1960) 2717.
[17] D.L. Reger, R.F. Semeniuc, M.D. Smith, Cryst. Growth Des. 5 (2005) 1181.
[18] M. Brookhart, B. Grant, A.F. Volpe, Jr., Organometallics 11 (1992) 3920.
[19] C.R. South, M.N. Higley, K.C.-F. Leung, D. Lanari, A. Nelson, R.H. Grubbs, J.F. Stoddart, M. Weck, Chem. Eur. J. 12 (2006) 3789.
[20] Crystal Structure: Crystal Analysis Package. Rigaku and Rigaku/MSC, 2000–2010.